Prediction of rheometrical and complex flows of entangled linear polymers using the DCR model with chain stretch*

Peter Wapperom†
Department of Mathematics, Virginia Tech, Blacksburg, Virginia 24061

Roland Keunings
CESAME, Division of Applied Mechanics, Université catholique de Louvain, B-1348 Louvain-la-Neuve, Belgium

Giovanni Ianniruberto
Department of Chemical Engineering, University Frederico II, Piazzale Tecchio, 80125 Napoli, Italy

(November 16, 2005)

Abstract

We study the rheometrical and complex flow response of the double-convection-reptation (DCR) model with chain stretch proposed recently by Ianniruberto and Marrucci (2002) for entangled linear polymers. The single- and two-mode differential versions of the model are used, with parameter values identified by Ianniruberto and Marrucci (2002) for a nearly monodisperse polybutadiene solution. These authors found that the DCR model with stretch predicts well the rheometrical shear behavior of the fluid in the modest experimental range of deformation rates. Our calculations for the higher shear rates reached in the simulations of complex flow reveal anomalous or questionable behavior, namely shear-thickening over an intermediate range of shear rates and large chain stretch reached in fast shear flows. This behavior is shown to be shared by the original integro-differential DCR theory, of which the differential DCR model is actually a mathematical approximation. We also show that the original DCR theory with stretch predicts excessive shear-thinning at high shear rates, while its differential approximation remains stable for all shear rates. Using the Backward-tracking Lagrangian particle method [Wapperom *et al.* (2000)], we investigate the response of the differential DCR model in start-up flow through an axisymmetric contrac-

*Dedicated to Professor G. Marrucci on the occasion of his 65th birthday

†Author to whom correspondence should be addressed; electronic mail: wapperom@math.vt.edu

tion/expansion geometry. We compare the single- and two-mode model predictions (in terms of steady-state vortex structure, chain stretch, and overall pressure drop), and correlate these with the steady and start-up rheometrical responses in shear and extension. Significant chain stretch is predicted in the vicinity of the axis of symmetry and in thin boundary layers located at the constriction wall. As a result, the DCR predictions significantly depart from the stress-optical rule in these flow regions. Chain stretch also affects the flow kinematics, with the appearance of a large upstream steady-state vortex. Surprisingly, however, the predicted pressure drop is not much affected by these kinematical changes, and is qualitatively described by a simple inelastic, shear-thinning model.

I. INTRODUCTION

The development of a definitive molecular-based constitutive theory for entangled linear polymers has known exciting advances over the last few years. The most successful models are extensions of the classical reptation theory [Doi and Edwards (1986)], with much of the progress being due to the creative efforts of Professor G. Marrucci. In particular, he recognized the importance of flow-induced constraint release effects, introducing the convective constraint release (CCR) mechanism [Marrucci (1996)].

In a recent paper, Ianniruberto and Marrucci (2001) developed a single-mode constitutive theory known as the double-convection-reptation (DCR) model, which accounts for CCR and stretch effects. The original DCR theory involves an integral equation for the average orientation of tube segments, and a differential equation for the average chain stretch. The characteristic time for orientational relaxation depends in a series-parallel way on three basic mechanisms, namely reptation, constraint release (both thermal and convective), and Rouse relaxation. Constraint release is assumed to have no impact on chain stretch. Furthermore, an alternative strain measure [Marrucci *et al.* (2001)] based on a force balance on the entanglement nodes is used in the integral orientation equation in order to obtain a simpler, differential form. In a companion paper, Ianniruberto and Marrucci (2002) proposed a multi-mode version of the differential DCR model with stretch, which involves a spectrum of disengagement and Rouse times. Using only two modes, the multi-mode theory was shown to yield already much improved predictions for the linear and non-linear shear response of monodisperse polymers.

The goal of the present work is to study by way of numerical simulation the response of the DCR model with stretch in start-up flow through an axisymmetric contraction/expansion geometry. The numerical technique is the Backward-tracking Lagrangian particle method [Wapperom *et al.* (2000)], which we have used previously to simulate complex flows of entangled linear and branched polymers [Wapperom and Keunings (2000, 2001)]. We consider the single- and two-mode DCR models, using parameter values identified by Ianniruberto and Marrucci (2002) for a nearly monodisperse polybutadiene solution. Since the range of deformations spanned by the numerical simulations is much wider than that considered by Ianniruberto and Marrucci (2002), it is useful to investigate in more detail the rheometrical response of the model. Interestingly, we find that the DCR theory predicts anomalous shear-thickening and large chain stretch in fast shear flows. These features are found both in the original integro-differential model, and its differential approximation. Moreover, the integro-differential model shows excessive shear-thinning at high shear rates, while the differential form has a monotonic flow curve. In view of these results, the complex flow simulations are reported for the differential version of the DCR theory. We compare the single- and two-mode model predictions at steady-state, in terms of vortex structure, molecular stretch, and pressure drop, and correlate these results with the rheometrical response in shear and extension. Simulations reported by Wapperom and Keunings (2000) with the MGI model, an earlier version of the theory that ignores chain stretch [Marrucci *et al.* (2001)]), show a continuous decrease of the upstream vortex with increasing Weissenberg number. The present results reveal that chain stretch has a significant impact on flow kinematics, leading eventually to a dramatic growth of the upstream vortex.

II. THE SINGLE- AND MULTI-MODE DCR MODELS WITH STRETCH

The single-mode DCR model with stretch proposed by Ianniruberto and Marrucci (2001) includes an evolution equation for the average tube orientation $\boldsymbol{S}$ and a separate evolution equation for the average chain stretch λ. The original orientation equation is of integral type, with a strain measure derived from a simple 3-chain model obeying force balance at the entanglement nodes. This integral equation is conveniently approximated by the following differential equation for the square of the orientation tensor [Marrucci *et al.* (2001)]:

$$\frac{D\boldsymbol{S}^2}{Dt} = \boldsymbol{\kappa}\cdot\boldsymbol{S}^2 + \boldsymbol{S}^2\cdot\boldsymbol{\kappa}^T - 2\boldsymbol{S}^2\left(\boldsymbol{\kappa}:\boldsymbol{S}\right) - \frac{2}{\tau}\left(\boldsymbol{S}^2 - \frac{1}{3}\boldsymbol{S}\right). \tag{1}$$

Here, D/Dt denotes the material derivative and $\boldsymbol{\kappa}$ is the transpose of the velocity gradient. The right-hand side of Eq. (1) consists of a convective part and a term that describes relaxation. The effective relaxation time τ is given by

$$\tau = \frac{1}{2\left(\frac{1}{\tau_\mathrm{d}} + |\boldsymbol{\kappa}:\boldsymbol{S}|\right)} + \tau_\mathrm{R}. \tag{2}$$

This formulation accounts for reptation (through the reptation time τ_d), for CCR (through $|\boldsymbol{\kappa}:\boldsymbol{S}|$), and for the intrinsic friction of the chain (through the Rouse time τ_R). The factor of 2 appearing in Eq. (2) expresses double reptation and CCR2. For slow flows, reptation dominates and $\tau \approx \tau_\mathrm{d}/2 + \tau_\mathrm{R}$ ($\approx \tau_\mathrm{d}/2$ for well entangled polymers). For faster flows, CCR decreases the relaxation time τ. Note that the absolute value must be included in the CCR contribution to assure a positive relaxation time. Indeed, in reversing flows, the velocity gradient changes sign instantaneously, while the orientation has a finite relaxation time, causing $\boldsymbol{\kappa}:\boldsymbol{S}$ to become negative [Wapperom and Keunings (2000)]. For very fast flows, when $|\boldsymbol{\kappa}:\boldsymbol{S}| \gg 1/\tau_\mathrm{d}$, τ reaches a non-vanishing minimum value equal to the Rouse time τ_R. (This is in contrast with the MGI model [Marrucci *et al.* (2001)] for which τ approaches zero at high flow rates, thus causing an almost instantaneous response.)

At flow rates larger than the reciprocal Rouse time, polymer chains get stretched. This is described by a separate evolution equation for the average stretch ratio λ,

$$\frac{D\lambda}{Dt} = \lambda\boldsymbol{\kappa}:\boldsymbol{S} - \frac{\lambda_\mathrm{max}}{\tau_\mathrm{R}}\frac{\lambda-1}{\lambda_\mathrm{max}-\lambda}. \tag{3}$$

The chain stretch is unity at equilibrium and has an upper limit λ_max. The latter is equal to the square root of the number of Kuhn steps between consecutive entanglements at equilibrium. The first term on the right-hand side of Eq. (3) accounts for affine convection of the chain, while the second describes stretch relaxation with the Rouse time taken as characteristic time.

Finally, the polymer stress $\boldsymbol{T}$ and refractive index $\boldsymbol{n}$ are related to the stretch λ and orientation $\boldsymbol{S}$ by the following algebraic relations:

$$\boldsymbol{T} = G\lambda^2\frac{\lambda_\mathrm{max}-1}{\lambda_\mathrm{max}-\lambda}\boldsymbol{S}, \tag{4}$$

$$\boldsymbol{n} = K\lambda^2\boldsymbol{S}. \tag{5}$$

Here, G is the shear modulus and K the corresponding optical quantity. The single-mode DCR theory thus has four material parameters (G, $\lambda_{\max}$, $\tau_{\rm d}$, $\tau_{\rm R}$), which can in principle all be determined from linear viscoelastic data. It should be noted that the model obeys the stress-optical rule only when the stretch is much smaller than $\lambda_{\max}$. We shall come back to this point in Sec. VI where we discuss simulation results in a complex flow geometry.

The single-mode DCR theory assumes that all chain segments behave in the same way. In the multi-mode version of the DCR model [Ianniruberto and Marrucci (2002)], chain segments are classified in N categories, each having their own characteristic disengagement and Rouse times. In particular, this enables to distinguish between internal chain segments (which relax by reptation) and segments at the end of the chain (which disengage by fluctuation). Constraint release (thermal and convective) gives rise to interactions between the different categories of segments. This is taken into account in the theory through N^2 orientation tensors $\boldsymbol{S}_{ij}$ pertaining to segments of type i that are entangled with segments of type j. The final set of equations proposed by Ianniruberto and Marrucci (2002) reads

$$\frac{D\boldsymbol{S}_{ij}^2}{Dt} = \boldsymbol{\kappa}\cdot\boldsymbol{S}_{ij}^2 + \boldsymbol{S}_{ij}^2\cdot\boldsymbol{\kappa}^T - 2\boldsymbol{S}_{ij}^2\,(\boldsymbol{\kappa}:\boldsymbol{S}_{ij}) - \frac{2}{\tau_{ij}}\left(\boldsymbol{S}_{ij}^2 - \frac{1}{3}\boldsymbol{S}_{ij}\right), \tag{6}$$

$$\tau_{ij} = \frac{1}{\left(\frac{1}{\tau_{{\rm d}i}} + \frac{1}{\tau_{{\rm d}j}} + |\boldsymbol{\kappa}:\boldsymbol{S}_i| + |\boldsymbol{\kappa}:\boldsymbol{S}_j|\right)} + \tau_{{\rm R}i}, \tag{7}$$

$$\boldsymbol{S}_i = \sum_{j=1}^{N} w_j \boldsymbol{S}_{ij}, \tag{8}$$

$$\frac{D\lambda_i}{Dt} = \lambda_i\boldsymbol{\kappa}:\boldsymbol{S}_i - \frac{\lambda_{\max}}{\tau_{{\rm R}i}}\frac{\lambda_i - 1}{\lambda_{\max} - \lambda_i}, \tag{9}$$

$$\boldsymbol{T} = G\sum_{i=1}^{N} w_i\lambda_i^2\frac{\lambda_{\max} - 1}{\lambda_{\max} - \lambda_i}\boldsymbol{S}_i, \tag{10}$$

$$\boldsymbol{n} = K\sum_{i=1}^{N} w_i\lambda_i^2\boldsymbol{S}_i. \tag{11}$$

Here, w_i is the mass fraction of chain segments of type i, while $\boldsymbol{S}_i$ and λ_i are their average orientation and stretch, respectively. The multi-mode DCR theory thus requires N^2 equations to describe orientation and N equations to describe stretch. It involves $3N + 2$ parameters, namely the shear modulus G, the maximum stretch $\lambda_{\max}$ (which is the same for all segment types), the set of N fractional weights w_i, and the N disengagement and Rouse times, $\tau_{{\rm d}i}$ and $\tau_{{\rm R}i}$. In principle, however, all such times can be related one to another, so that one basic time scale only must be specified [Ianniruberto and Marrucci (2002)].

III. FLUID PARAMETERS AND RHEOMETRICAL RESPONSE

Ianniruberto and Marrucci (2002) used the DCR theory with stretch to describe the experimental shear data obtained by Menezes and Graessley (1982) for a 7.5% by volume solution of nearly monodisperse polybutadiene ($M_w = 350,000$) in a commercial hydrocarbon oil. It was found that use of a two-mode model ($N = 2$) instead of the single-mode model ($N = 1$) already improves the predictions significantly. For the single-mode theory,

a fit of the steady-state data for the shear stress and first normal stress difference yields the following parameter values: $G = 9000$ Pa, $\tau_d = 1.5$ s, $\tau_{\rm R} = 0.5$ s, and $\lambda_{\rm max} = 2.5$. For the two-mode model, Ianniruberto and Marrucci (2002) distinguish between internal segments (index 1) that relax slowly, and end segments (index 2) that relax much faster. All parameters are identified by fitting the linear viscoelastic data, with the exception of the maximum stretch which is estimated from the number of Kuhn segments between consecutive entanglements at equilibrium. This yields the following values: $G = 19,800$ Pa, $w_1 = 0.65$ (hence $w_2 = 0.35$), $\lambda_{\rm max} = 10$, $\tau_{d1} = 2.1$ s, $\tau_{d2} = 0.08$ s, $\tau_{\rm R1} = 0.12$ s, $\tau_{\rm R2} = 0$. A vanishing second Rouse time implies that the stretch λ_2 remains equal to its equilibrium value, $\lambda_2 = 1$. The steady-state data for shear stress and first normal stress difference of Menezes and Graessley (1982) are well described with both the single- and double-mode parameter sets. The two-mode model provides, however, a much better prediction of the start-up shear stress data, particularly at short times.

For our simulations of the flow through the constriction, we shall adopt the above parameters so as to guarantee that the single- and two-mode versions of the DCR model give essentially undistinguishable results in steady shear flow, at least in the shear rate window of the experiments by Menezes and Graessley (1982). One should point out that the experimental data are only available up to shear rates of order 20 $\rm s^{-1}$. The value of the maximum stretch $\lambda_{\rm max}$ is in fact rather inconsequential for such modest shear rates. It does, however, have a great impact in the simulation results for the constriction flow. Indeed, as discussed in Sec. VI, the deformation rates that develop in the wall boundary layers are of the order of 100 to 200 $\rm s^{-1}$. This induces significant levels of chain stretch (and thus of polymer stress), which are indeed very sensitive to the actual value of $\lambda_{\rm max}$.

In order to better understand the behavior in complex flow, we first discuss the differences in rheometrical flow response between the single- and two-mode models for the above parameter values. We shall limit ourselves to those quantities that are most relevant for the flow through an axisymmetric constriction. All rheometrical results have been obtained with a simplified version of the numerical method that we discuss briefly in section V, in order to verify the numerical implementation of the models.

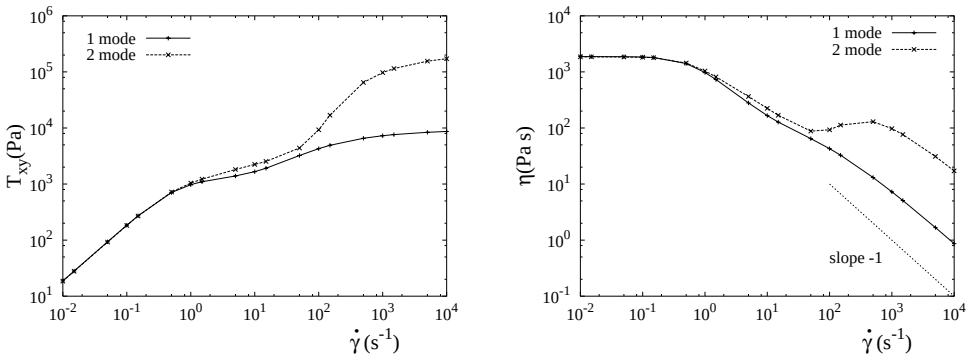

(a) (b)

FIG. 1. Steady-state shear response of the single- and two-mode DCR models with stretch, using parameter values obtained by Ianniruberto and Marrucci (2002): (a) shear stress T_{xy}, and (b) shear viscosity η as a function of shear rate $\dot{\gamma}$.

As shown in Fig. 1(a), the steady-state shear stress T_{xy} is identical for both models at low shear rates. At intermediate shear rates, when CCR dominates, the shear stress for the two-mode model is only slightly larger. For shear rates larger than $\dot{\gamma} \approx 50$ s^{-1}, however, chain stretch is significant and the predictions become sensitive to the value of the maximum stretch. Since the shear stress eventually reaches a plateau value which is proportional to the square of $\lambda_{\max}$ [Ianniruberto and Marrucci (2002)], differences between the single- and two-mode results are substantial indeed.

In Fig. 1(b), we compare the corresponding steady-state shear viscosities. Although merely a scaling of the shear stress axis by the shear rate, the viscosity curves show some properties that cannot readily be observed from the stress plot. First, we observe that the slope at high shear rates always remains larger than -1. Second, the two-mode DCR model predicts shear-thickening behavior at deformation rates between 10^2 and 10^3 s^{-1}, which clearly is physically unrealistic. On the other hand, the single-mode theory predicts a small change in slope at somewhat lower rates, but it does not show shear-thickening. The reason is mainly due to the very different values of $\lambda_{\max}$. This can be understood from Fig. 2(a), where chain stretch is displayed as a function of shear rate. We observe that the one-mode version stretches earlier, but the change from the equilibrium value of 1 to the maximum $\lambda_{\max} = 2.5$ is rather gradual. For the two-mode version, however, stretching occurs at higher flow rates and the transition from 1 to $\lambda_{\max} = 10$ is much steeper. The nonlinear multiplicative factor involving λ in the stress equation (10) increases faster with shear rate than S_{xy} decreases, resulting in an increasing viscosity. Prediction of shear-thickening behavior for a range of shear rates is a general problem of the DCR theory, which would also occur with the single-mode version should a larger value of $\lambda_{\max}$ be used.

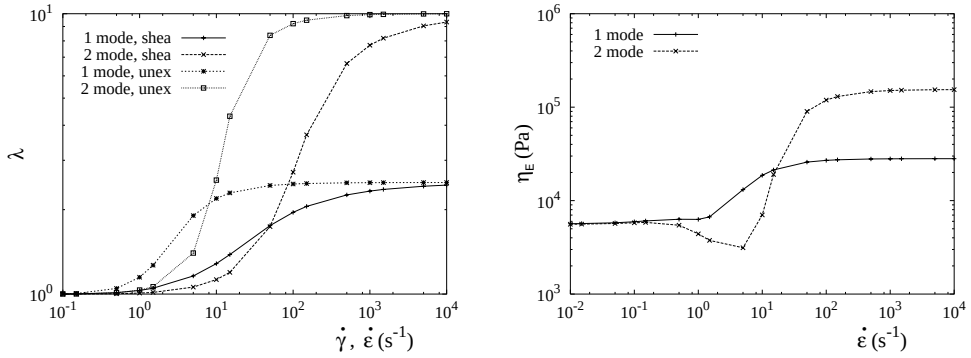

(a) (b)

FIG. 2. Single- and two-mode DCR models with stretch: (a) chain stretch λ in steady-state shear and uniaxial extension, and (b) elongational viscosity $\eta_{\rm E}$ as a function of deformation rate $\dot{\gamma}$ or $\dot{\epsilon}$.

We also observe from Fig. 2(a) that the chain stretch predicted by the DCR theory eventually reaches the maximum stretch $\lambda_{\rm max}$ at high shear rates. Whether this is physically realistic is an open question. The results for uniaxial extension are very similar to those for shear flow, except that chain stretch in elongation occurs at lower deformation rates, as expected. The maximum stretch is reached asymptotically as well, but this of course makes sense in extension. The corresponding results for the extensional viscosity are depicted in Fig. 2(b). As for the shear viscosity, a difference in plateau value is observed which is caused by the difference in maximum stretch. (Indeed, the plateau extensional viscosity is also proportional to the square of $\lambda_{\rm max}$.) A second difference is observed at intermediate elongation rates. With the two-mode model, since chain stretch occurs at higher elongation rates than with the single-mode version, the extensional viscosity first decreases due to CCR before showing an increase due to chain stretch. The CCR-dominated decrease in extensional viscosity is similar to the behavior of the MGI model discussed by Wapperom and Keunings (2001). Since the latter model does not include stretch and has a vanishing effective relaxation time at high deformation rates, its extensional viscosity decreases monotonically.

We conclude our discussion of the DCR steady-state rheometrical response with results for the first normal stress difference N_1 and stress ratio $S_{\rm R}$ in shear flow. The latter is a measure of the fluid's elasticity. It is defined as

$$S_{\rm R} = \frac{N_1}{2T_{xy}}. \tag{12}$$

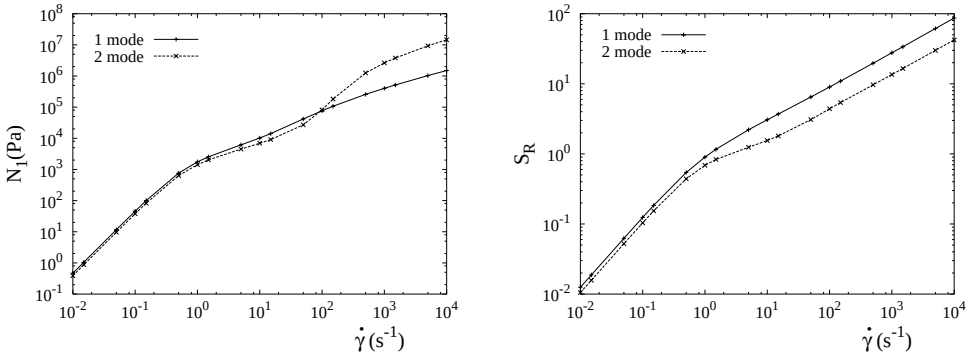

(a) (b)

FIG. 3. Single- and two-mode DCR models with stretch: (a) first normal stress difference N_1, and (b) stress ratio S_{R} as a function of shear rate $\dot{\gamma}$.

Single- and two-mode results for N_1 are very similar until chain stretch comes into play, again due to the different values of $\lambda_{\max}$. At large shear rates, N_1 becomes proportional to $\dot{\gamma}^{1/2}$. The corresponding stress ratio results are shown in Fig. 3(b). For both models, S_R increases monotonically. It is proportional to $\dot{\gamma}$ at small shear rates, and to $\dot{\gamma}^{1/2}$ at large shear rates, like N_1. For the one-mode model, the transition occurs quite abruptly, while the two-mode model tends to reach a plateau before showing its asymptotic behavior. We note for further reference that, in view of the larger stress ratio, a lower maximum Weissenberg number is expected to be reached in complex flow simulations with the single-mode model.

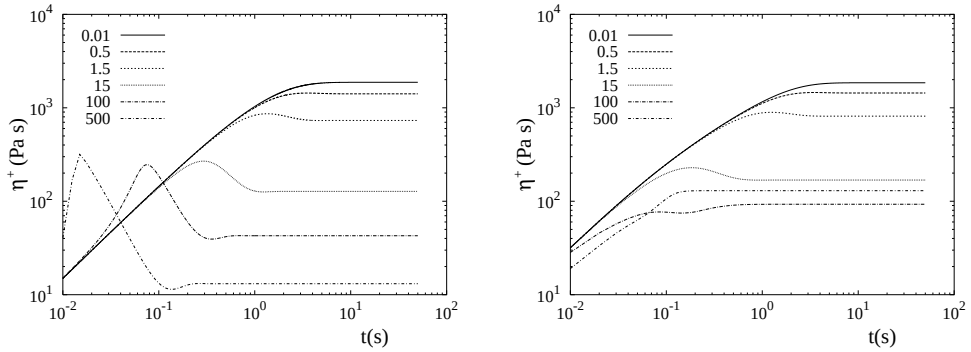

(a) (b)

FIG. 4. Transient shear viscosity η^+ as a function of time t for imposed deformation rate between 0.01 and 500 s^{-1}: (a) single-mode and (b) two-mode DCR models with stretch.

Finally, we briefly compare the stress response in start-up of shear and uniaxial elongation. The transient shear viscosity η^+ is depicted in Fig. 4. For low and intermediate shear rates, the stress growth at short times is considerably faster for the two-mode model due to the smaller disengagement time of the second mode. At these deformation rates, both models predict a small overshoot before the steady-state value is reached. For high shear rates, however, the single-mode model shows overshoots of increasing amplitude, while these

overshoots disappear completely with the two-mode model.

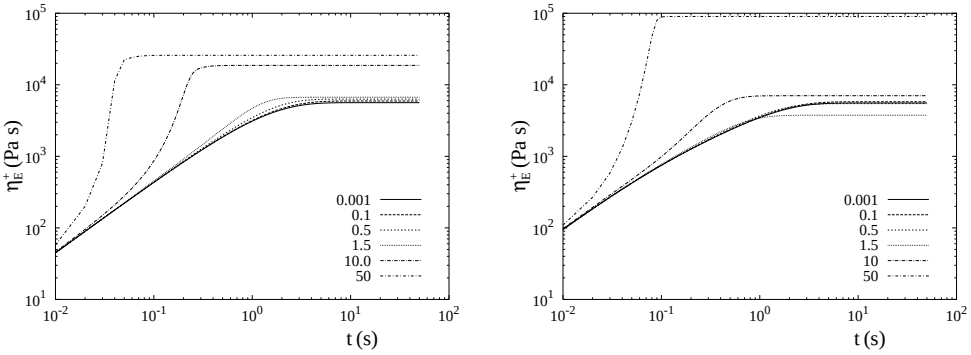

(a) (b)

FIG. 5. Transient uniaxial elongational viscosity η_{E}^{+} as a function of time t for imposed deformation rate between 0.001 and 50 s^{-1}: (a) single-mode and (b) two-mode DCR models with stretch.

Results for the transient extensional viscosity η_{E}^{+} depicted in Fig. 5 show strain-hardening due to chain stretch, before reaching a steady-state value. The latter is reached ever faster with increasing deformation rate. Here again, differences between the single- and two-mode results are mainly due to the different values of $\lambda_{\max}$. As for the transient shear response, the stress growth at short times is considerably faster for the two-mode model.

IV. IMPACT OF THE DIFFERENTIAL APPROXIMATION

As noted earlier, the differential evolution equation (1) for the orientation tensor is actually a mathematical approximation of the original, DCR integral equation [Ianniruberto and Marrucci (2001)]. At this point, it is appropriate to investigate whether the anomalous or questionable behavior of the DCR model discussed in the previous section (i.e. shear-thickening for a range of shear rates and large chain stretch reached in fast shear flows) is really intrinsic to the DCR theory or an artifact of the approximation process. In the original DCR theory, the average orientation at present time t is given by the memory integral

$$\boldsymbol{S} = \int_{-\infty}^{t} \mu(t;t')\boldsymbol{Q}(t;t')\ \mathrm{d}t', \tag{13}$$

with a memory function $\mu(t;t')$ defined as

$$\mu(t;t') = \frac{1}{\tau(t')} \exp\left(-\int_{t'}^{t} \frac{\mathrm{d}t''}{\tau(t'')}\right). \tag{14}$$

Here, the effective relaxation time τ is defined by Eq. (2), as for the differential version. The orientation tensor $\boldsymbol{Q}$ takes the form

$$\boldsymbol{Q} = \frac{\sqrt{\boldsymbol{B}}}{\mathrm{tr}\ \sqrt{\boldsymbol{B}}}, \tag{15}$$

where $\boldsymbol{B}$ denotes the Finger strain tensor. The latter evolves according to

$$\frac{D\boldsymbol{B}}{Dt} = \boldsymbol{\kappa}\cdot\boldsymbol{B} + \boldsymbol{B}\cdot\boldsymbol{\kappa}^T. \tag{16}$$

The equations governing chain stretch and stress are the same as in the previous section. The full set of equations is thus of integro-differential form.

In order to compare the integral and differential versions of the DCR model, we consider the single-mode theory using the same parameter values as before (in particular, $\lambda_{\max} = 2.5$).

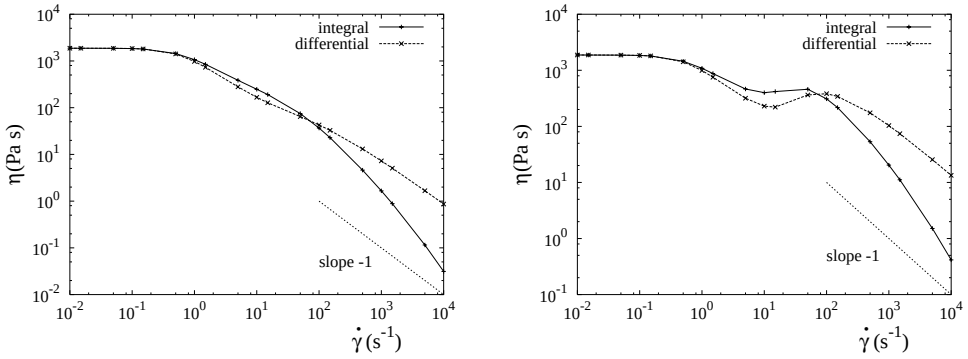

(a) (b)

FIG. 6. Steady-state shear viscosity for the single-mode integral and differential DCR models with stretch: (a) $\lambda_{\max} = 2.5$, (b) $\lambda_{\max} = 10$.

The impact of the differential approximation on the steady shear viscosity is shown in Fig. 6(a). In the range of shear rates where CCR is active, the integral and differential models are in good agreement. This agreement comes to no surprise, and indeed it was already noticed in absence of chain stretch, in both rheometrical and complex flows [Marrucci *et al.* (2001); Wapperom and Keunings (2000)]. For larger shear rates such that the effective relaxation time τ reaches the Rouse time, however, the integral model shows excessive shear-thinning. The logarithmic slope of the viscosity curve becomes very quickly smaller than -1, which implies a material instability and would limit computations in complex flow geometries to moderate values of the Weissenberg number.

A larger value of the maximum chain stretch does not prevent the excessive shear-thinning predicted by the original integral DCR model. This can be seen in Fig. 6(b), where we compare the single-mode differential and integral models for $\lambda_{\max} = 10$. From this figure, it also becomes apparent that anomalous shear-thickening behavior is predicted for large (but physically relevant) values of $\lambda_{\max}$, and that it is not an artifact of the differential approximation.

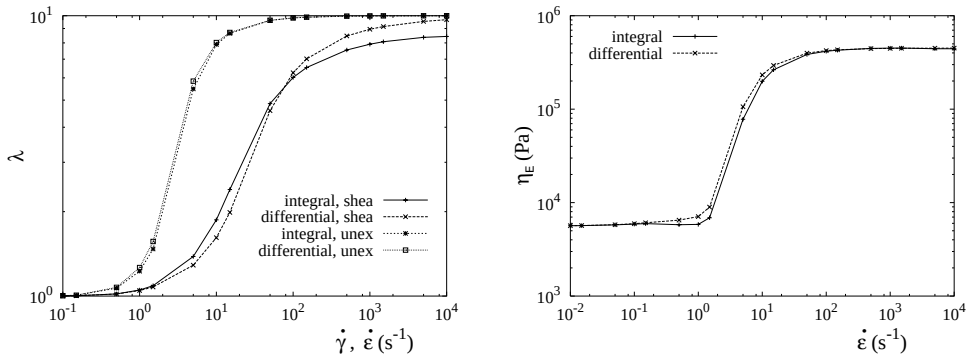

(a) (b)

FIG. 7. Single-mode integral and differential DCR models with stretch: (a) chain stretch in steady-state shear and uniaxial extension, and (b) steady uniaxial elongational viscosity $\eta_{\rm E}$ ($\lambda_{\rm max} = 10$).

Results for the chain stretch are shown in Fig. 7(a). In shear, the integral model also predicts that chain stretch approaches $\lambda_{\rm max}$ at high deformation rates, although not as fast as the differential approximation. This particular result is thus intrinsic to the DCR theory with stretch. In uniaxial extension, the predicted stretch curves are in excellent agreement indeed. This also holds true for the corresponding elongational viscosity, shown in Fig. 7(b).

Similar results would be obtained with the multi-mode version of the theory. We thus conclude that predictions of shear-thickening behavior and large chain stretch in fast shear flows are not an artifact of the differential approximation for the orientation equation. Also, the original integral DCR model shows excessive shear-thinning at shear rates for which chain stretch is dominant. This difficulty is not found with the differential approximation. Improvement of the theory is clearly needed, and we shall return to this point in the conclusion section.

The above results suggest several other considerations. First, they reveal that it is not easy to derive a differential version really equivalent to a given integral constitutive equation. We know that this derivation requires some mathematical approximations in the general case, while only very simple integral equations (e.g., the Lodge equation) have an exact differential equivalent (i.e., the upper-convected Maxwell model). More complex equations, such as the integral DCR model, only have a differential "analogue". The differential form (1) proposed by Marrucci *et al.* (2001) was derived using a procedure suggested by Larson (1987). It consists in first looking for a differential form exactly equivalent to the integral equation for the limiting case of a deformation jump. (Even this initial calculation step is not necessarily successful. For instance, there is apparently no hope if the integral contains the Doi–Edwards $\boldsymbol{Q}$ tensor, while it is successful with the simpler $\boldsymbol{Q}$ tensor (15) adopted by Marrucci *et al.* (2001); the latter is nonetheless a very good approximation of the Doi–Edwards $\boldsymbol{Q}$ tensor!) The procedure is then completed by adding to the differential equation a relaxation term which reduces to a simple exponential in the linear limit, as is the case for the integral equation. Although this procedure guarantees that the integral and differential equations are essentially equivalent in slow or even moderately fast flows, it does not assure that the two equations remain alike (not even qualitatively) in highly non-linear situations.

The matter definitely requires further investigation.

Finally, the discrepancies at very high shear rates between the integral and differential equations for the orientation tensor are not only a mathematical issue. As is apparent from Fig. 6, the integral equation predicts an instability in very fast shear flows, while the differential equation is stable. To understand such a difference in behavior, we first note that, when chains start to be stretched, they abandon the CCR-induced plateau value of the orientation, eventually becoming fully oriented along the flow direction. However, if chains tend to align slowly enough, stretch effects can compensate for the orienting action. The difference between the integral and differential equation lies just on the way in which chains are predicted to orient along the flow direction. Indeed, in the high shear rate limit, the differential equation gives S_{xy} proportional to $\dot{\gamma}^{-1/2}$, while the integral equation gives a steeper slope, i.e., S_{xy} nearly proportional to $\dot{\gamma}^{-0.9}$. In the differential case, orientation and stretch effects exactly balance each other, generating a shear stress plateau (following that due to CCR), while in the integral case, the orientation effect dominates, thus inducing an instability.

V. COMPLEX FLOW: NUMERICAL METHOD AND PROBLEM DESCRIPTION

We now turn to simulations of a complex flow. We have indeed performed simulations with the original integro-differential DCR theory, using methods similar to the ones implemented by Wapperom and Keunings (2000, 2001) for the MGI and pom-pom models. In view of the excessive shear-thinning of the original theory, however, these very intricate simulations are limited to moderate values of the Weissenberg number. They will not be reported here. In the sequel, we shall exclusively use the differential version of the DCR theory.

In the simulation of complex flows, the constitutive equation is coupled with the conservation laws. Here, we consider incompressible, isothermal, and inertialess flow. The conservation laws for mass and linear momentum then reduce respectively to

$$\nabla \cdot \boldsymbol{v} = 0, \tag{17}$$

$$-\nabla p + \nabla \cdot \boldsymbol{T} = \boldsymbol{0}, \tag{18}$$

where $\boldsymbol{v}$ is the fluid velocity and p the hydrodynamic pressure. The polymeric stress $\boldsymbol{T}$ is given by either Eq. (4) or (10) for the single- and multi-mode versions of the DCR model, respectively. Note that Eq. (18) only contains the polymer stress and does not include any purely-viscous component.

The governing equations are solved with the Backward-tracking Lagrangian Particle Method developed by Wapperom *et al.* (2000) for solving transient viscoelastic flows using a macroscopic or micro-macro approach. At each time step, the Eulerian solution of the conservation laws is decoupled from the Lagrangian integration of the evolution equation for orientation and stretch. This allows us to use different solution methods for the conservation laws and the evolution equations. The equations of motion (17), (18) are discretized by means of the Galerkin finite element method. The Discrete Elastic-Viscous Stress Splitting (DEVSS) method [Guénette and Fortin (1995)] has been used to enhance stability of the numerical scheme. Here, the discontinuous velocity gradient is taken at time level $n + 1$,

while the continuous linear velocity gradient is taken at time level n, i.e. the same level as the viscoelastic stress. This guarantees a non-singular matrix when solving for the conservation laws. To obtain the polymer stress $\boldsymbol{T}$, we integrate the evolution equations for orientation and stretch along discrete particle trajectories. The main difference with other Lagrangian particle methods is that we track the motion of a particle backward in time. This allows us to directly evaluate the stress or stretch at pre-defined, fixed particle locations. At the same time, this minimizes the number of particles, so that CPU time and memory requirements are reduced considerably. A detailed description of the numerical method can be found in the precursor paper by Wapperom *et al.* (2000).

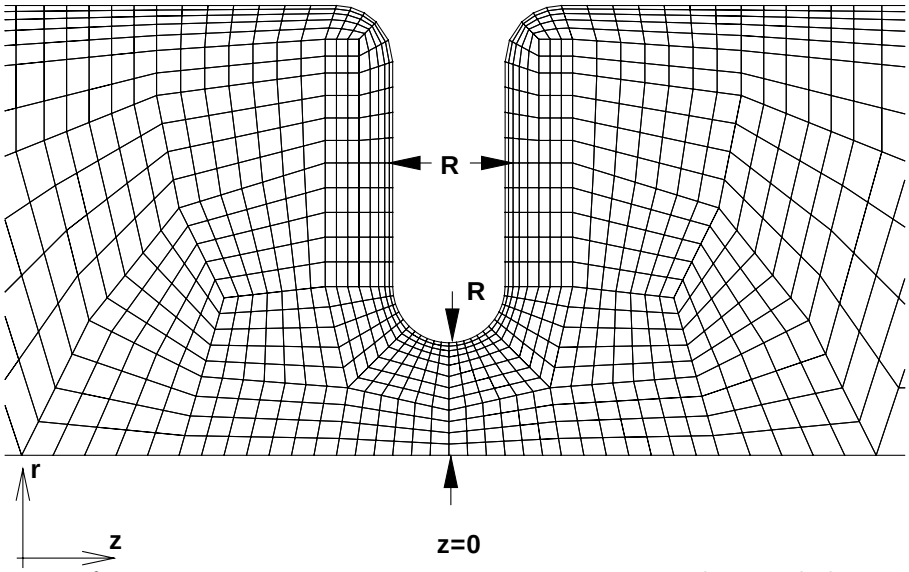

FIG. 8. Zoom of 4:1:4 axisymmetric constriction geometry with rounded corners and finite element mesh with medium level of refinement.

We consider the start-up flow through an axisymmetric 4:1:4 constriction with rounded corners, as depicted in Fig. 8. The smallest gap (at $z = 0$ in Fig. 8) has a radius R, while all rounded corners have radius of curvature $R/2$. The lengths of the inlet and outlet regions are equal to $19.5R$, and at both inlet and outlet we impose fully-developed velocity boundary conditions, which have been calculated separately. No-slip velocity boundary conditions are specified at the wall and symmetry conditions hold at the centerline.

The results shown below have been obtained with the "medium" mesh used by Wapperom and Keunings (2000, 2001) for the MGI and pom-pom models, for which it was shown to be sufficiently refined. That mesh, depicted in Fig. 8, contains 1288 quadrilateral elements and is particularly refined near the constriction wall where steep boundary layers may develop. The smallest element has an area of $\Omega_{\rm e} = 2.0 \cdot 10^{-3}$, scaled with R^2.

In all simulations, we consider creeping flow, so that, in the absence of a solvent viscosity, the characteristic dimensionless numbers are the Weissenberg numbers for orientation and stretch. Henceforth, we use the orientation Weissenberg number to characterize the flow. For the single-mode model, we use as fluid time scale the effective relaxation time at equilibrium, namely $\tau_0 = \tau_{\rm d}/2 + \tau_{\rm R}$. For the two-mode model, we use the largest equilibrium relaxation time, $\tau_0 = \tau_{\rm d1}/2 + \tau_{\rm R1}$ ($\tau_{\rm d2}$ is small compared to the first mode). The orientation Weissenberg number is now defined as $\mathrm{We} = \tau_0 U/R$, where U is the average velocity in the section of

smallest gap.

The calculations were performed on a single processor of an Origin 2000 with a 300 MHZ MIPS R12000 processor. Although the number of orientation tensors increases by a factor 4 by going from the single- to the two-mode DCR model, the CPU time only increased by 20 %. The reason for this is threefold. First, approximately 70 % of the time is spent in solving the equations of motion. The CPU time in the integration of the constitutive equations therefore only increases from 90 to 150 minutes when going from 1 to 4 configuration tensors. A major reason for this is that the particle trajectories and velocity gradients only need to be computed once. Finally, loading the local values of the configuration tensor can be done more efficiently. For the lower Weissenberg number calculations, this resulted in a total CPU time of approximately 5 hours or 1.8 seconds per time step.

VI. RESULTS OF CONSTRICTION FLOW SIMULATIONS

Although the flow problem is transient, we focus here on the steady-state regime obtained as the long-time limit of the simulations, starting from the equilibrium state. With the single-mode model, a stable steady-state was found up to We = 30, while we could reach We = 100 with the two-mode model.

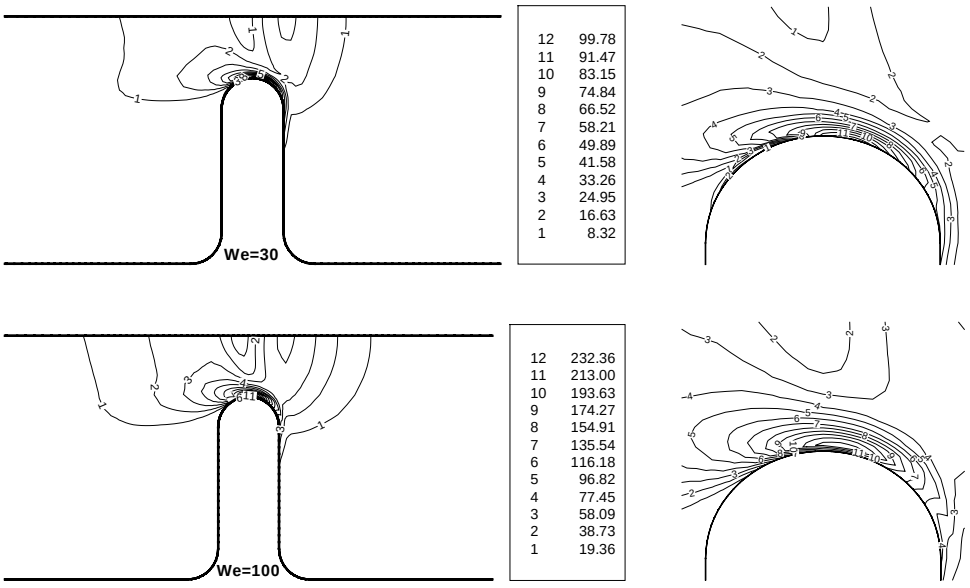

FIG. 9. Second invariant II_d of the rate-of-deformation tensor for the single-mode (We = 30; top figures) and two-mode (We = 100, bottom figures) DCR models with stretch. As in all similar figures to follow, the flow is from left to right, and a zoom of the constriction region is shown.

First, it is instructive to identify the range of deformation rates spanned by the simulations. In Fig. 9, we display contour lines of the second invariant $II_d = \sqrt{2\boldsymbol{d}:\boldsymbol{d}}$ of the rate-of-deformation tensor $\boldsymbol{d} = (\boldsymbol{\kappa} + \boldsymbol{\kappa}^T)/2$ for the highest Weissenberg numbers obtained. At the constriction wall, we have a pure shear flow and II_d reduces to the shear rate $\dot{\gamma}$. Along the axis of symmetry, the kinematics are that of uniaxial extension and II_d reduces to $\sqrt{3}\dot{\epsilon}$. Both the single- and two-mode models predict a thin boundary layer with high II_d values

at the constriction wall. As can be seen from the zooms, the main part of the boundary layer is located downstream, where the maximum value (of order 100 s^{-1}) is attained at the wall for the single-mode model, and slightly off the wall (of order 200 s^{-1}) for the two-mode model.

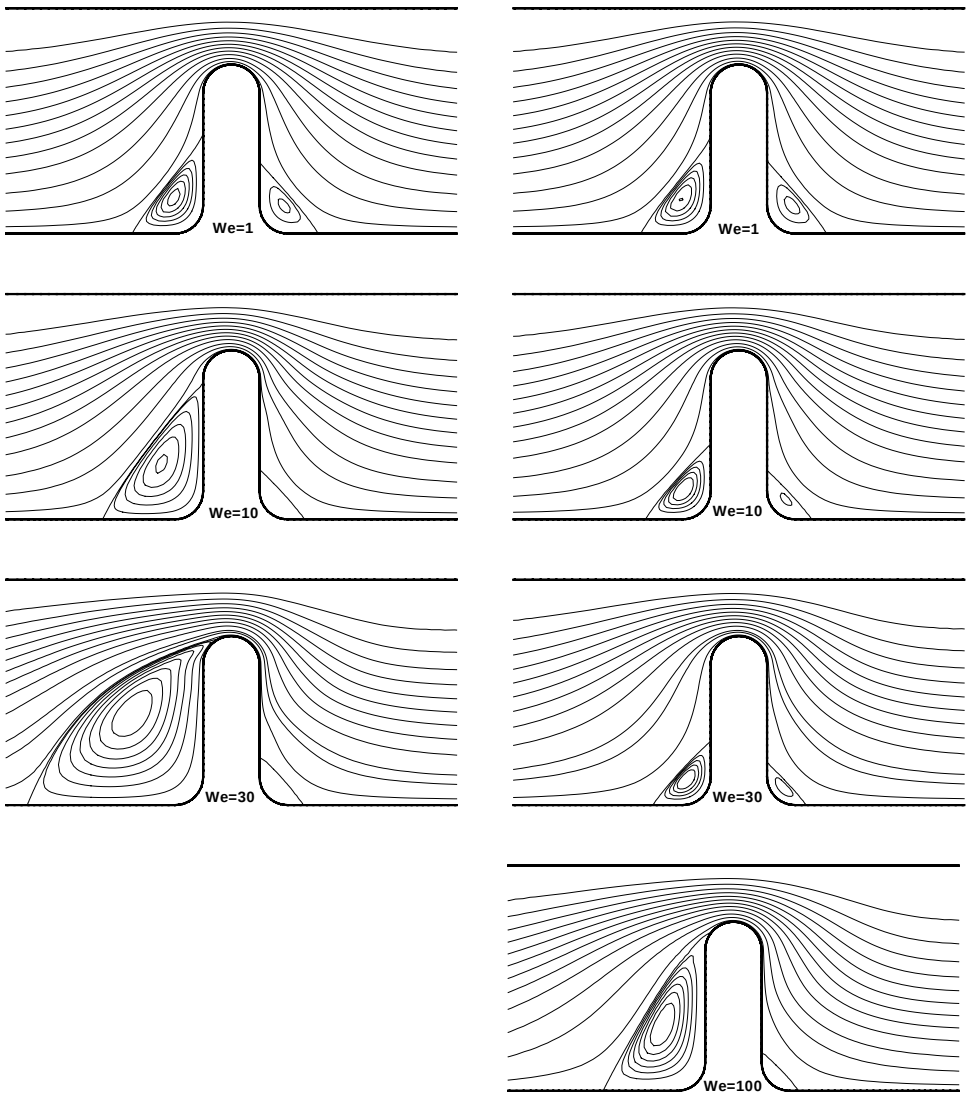

FIG. 10. Steady-state streamlines at various values of the Weissenberg number We for the single-mode (left) and two-mode (right) DCR model with stretch.

Characteristic of viscoelastic contraction flows is the appearance of vortices. In Fig. 10, we compare the steady-state streamlines obtained with the single- and two-mode DCR models. The streamline patterns at We = 1 show already a significant deviation from the inertialess Newtonian case, for which the streamlines would be symmetric about $z = 0$. For this relatively low Weissenberg number, the steady-state rheometrical responses are practically identical for both models, and the streamline patterns are almost indistinguishable as well. The impact of the higher transient shear and elongational viscosities at short times for the two-mode model appears to be minimal. At higher Weissenberg numbers, the predictions

of the downstream vortex are very similar, but the upstream vortices differ dramatically. This is consistent with the large differences in the extensional response of the two models at moderate and high deformation rates (cfr. Fig. 2(b)). For the single-mode model, there is already a significant growth of the upstream vortex at We = 10, which is due to chain stretch and the corresponding increase in extensional viscosity. For the two-mode model, the size of the upstream vortex decreases at first, in view of the CCR-dominated decrease of the extensional viscosity at intermediate deformation rates. At We = 30, the single-mode model shows a huge upstream vortex. The upstream vortex for the two-mode model, however, continues to decrease in size. Its eventual increase occurs only at much higher Weissenberg numbers, when chain stretch comes into play. At We = 100, the upstream vortex size is comparable to that predicted by the single-mode theory at We = 10. All these observations are indeed consistent with the rheometrical response of the two models in steady uniaxial extension. Note that the MGI model (which does include CCR but not chain stretch) shows a monotonic decrease of the size of the upstream vortex, while the integro-differential pom-pom model for branched polymers (which includes chain stretch) shows a vortex growth that is qualitatively similar to what is predicted by the DCR theory [Wapperom and Keunings (2000, 2001)].

When dealing with highly shear-thinning fluid models, it is always useful to compare the predictions of the complete viscoelastic theory with those of an inelastic, generalized Newtonian fluid (GNF) model having a similar viscosity curve. Here, we consider the Carreau–Yasuda GNF model [Bird *et al.* (1987)], whose shear viscosity is given by

$$\eta = \eta_0 \left(1 + [\lambda II_d]^a\right)^{(n-1)/a} . \tag{19}$$

The four adjustable parameters are the zero-shear-rate viscosity η_0, a time constant λ (which of course does not have the meaning of a relaxation time), the power-law index n, and a numerical parameter a.

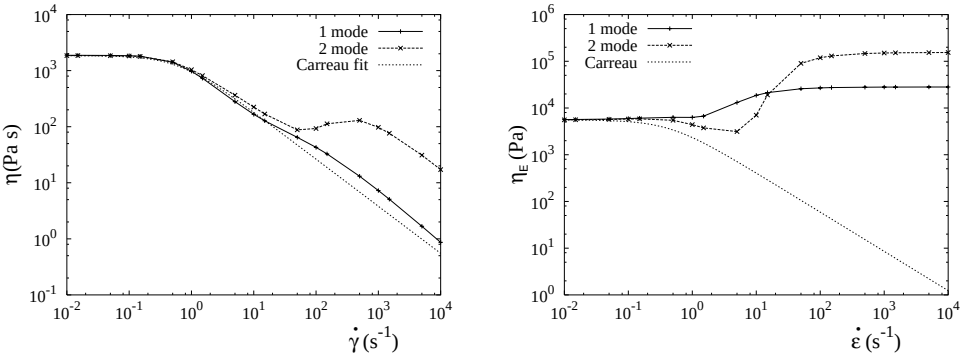

(a) (b)

FIG. 11. (a) Fit of DCR shear viscosity η with the Carreau–Yasuda inelastic model, and (b) corresponding prediction of extensional viscosity η_E.

We have identified the parameters of the Carreau–Yasuda model by fitting the shear viscosity of the single-mode DCR theory. The selected fit is shown in Fig. 11(a); it is obtained with the parameter values $\eta_0 = 1853$ Pa s, $\lambda = 1.58$ s, $n = 0.16$, and $a = 1.3$.

Note that the change in slope seen in the DCR results, caused by chain stretch, cannot be captured by the inelastic model, so that there is always a discrepancy in the fit, either for intermediate or large values of $\dot{\gamma}$. This particular fit has been chosen since high values of $\dot{\gamma}$ in shear deformations are only attained very locally in the constriction flow. Using these parameters, the elongational viscosity predicted by the inelastic model is shown in Fig. 11(b). As it should, it is similar to the shear viscosity curve. The DCR viscosity increase due to chain stretch cannot be described by the inelastic model. (This is in sharp contrast with the MGI model, which does not include a Rouse time and corresponding chain stretch. For this model, the elongational viscosity nearly coincides with the inelastic "prediction" as shown by Wapperom and Keunings (2000).)

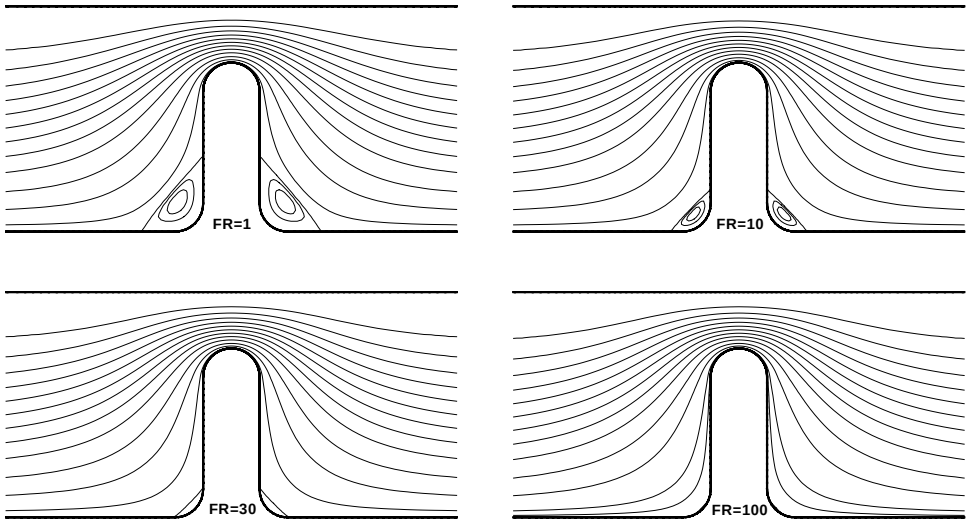

FIG. 12. Carreau–Yasuda inelastic model: steady-state streamlines as a function of dimensionless flow rate FR.

The steady-state streamlines computed with the inelastic Carreau–Yasuda model are displayed in Fig. 12, as a function of the dimensionless flow rate FR. The latter is defined such as to be directly comparable to the Weissenberg number for the viscoelastic results. The absence of elasticity (and of inertia) yields symmetric streamline patterns, and the monotonic elongation-thinning behavior of the Carreau–Yasuda model yields vortices of ever-decreasing size. The difference with the viscoelastic DCR results of Fig. 10 is striking indeed. This again is in sharp contrast with results obtained for the MGI model [Wapperom and Keunings (2000)].

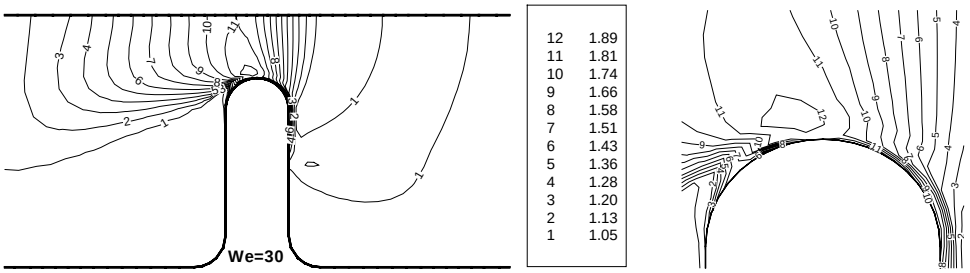

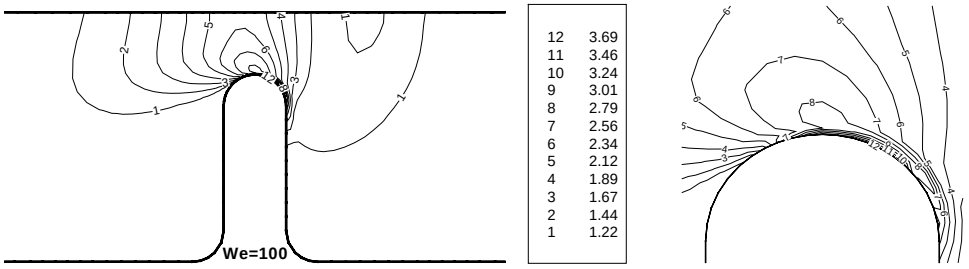

FIG. 13. Chain stretch λ for single-mode (We = 30; top figures) and two-mode (We = 100; bottom figures) DCR models.

We now go back to the DCR viscoelastic results, and report predictions for chain stretch. Results for the highest Weissenberg numbers are illustrated in Fig. 13. For both the single- and two-mode models, a stretch boundary layer develops near the constriction wall. As noted earlier, the large values of stretch predicted by the DCR theory in this shear-dominated region may not be physically realistic. For the single-mode model ($\lambda_{\max} = 2.5$), the polymers are also severely stretched in the extensional flow at the centerline (the stretch computed there is only slightly less than near the constriction wall). For the two-mode model ($\lambda_{\max} = 10$), polymers are much more stretched near the constriction wall than near the centerline.

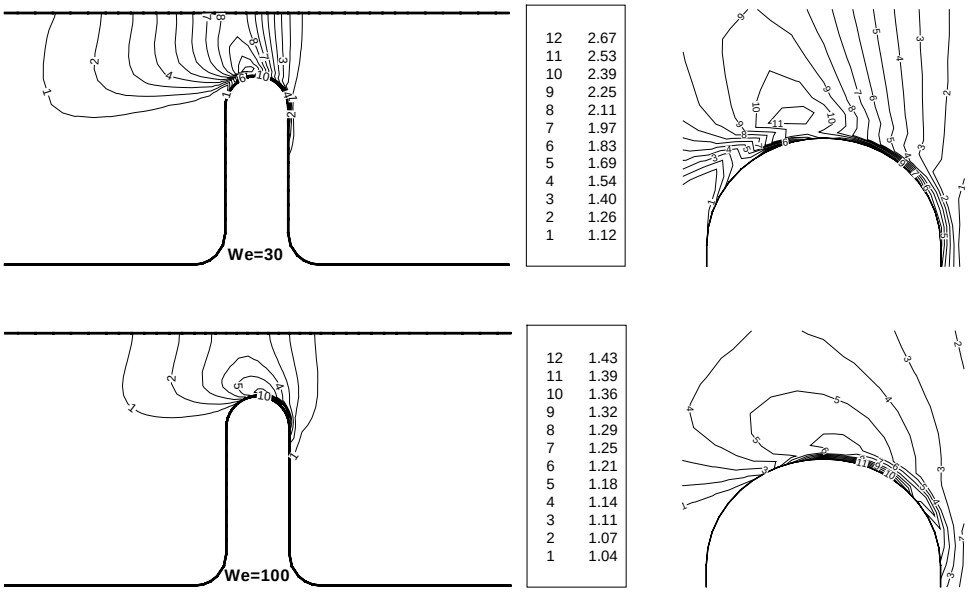

FIG. 14. Stress-optical ratio predicted by the single-mode (We = 30; top figures) and two-mode (We = 100; bottom figures) DCR models with stretch.

Experimentally, a common way of measuring stresses in complex flows of polymeric fluids is to take birefringence data and apply the stress-optical rule, assuming that it holds. Using the simulation results, we can readily quantify departures of the DCR theory from this rule. To do so, we compute the ratio of the non-dimensional stress $\boldsymbol{T}/G$ and the refractive index $\boldsymbol{n}/K$. The stress-optical rule holds if this ratio equals 1. Using Eqs. (4-5) for the single-mode model, we find that the stress-optical ratio reduces to the scalar

quantity $(\lambda_{\max} - 1)/(\lambda_{\max} - \lambda)$. Contour lines are displayed in Fig. 14. Clearly, deviation from the stress-optical rule is severe in a significant part of the flow domain, not only in the constriction region but also upstream. The stress-optical ratio is of order 2 at the centerline, where elongation dominates, while it reaches a value of 2.7 in the wall boundary layer where shear dominates (and where the large DCR stretch predictions are of questionable validity). Downstream of the constriction, stress and stretch relax fast so that the stress-optical ratio quickly recovers its equilibrium value of 1.

Eqs. (10-11) for the multi-mode model show that the stress-optical ratio does not reduce to a simple scalar factor. For the sake of illustration, the ratio depicted in Fig. 14 is calculated using the rr-components. Although the Weissenberg number is more than three times as large as for the single-mode model, the deviations from the stress-optical rule are much smaller. Also, they are mainly located in a boundary layer near the constriction wall. At the centerline, the maximum deviation is less than 15 %. The reason for this is that chain stretch for the single-mode model is relatively closer to its maximum value $\lambda_{\max}$ (see Fig. 13), which results in a large ratio $(\lambda_{\max} - 1)/(\lambda_{\max} - \lambda)$.

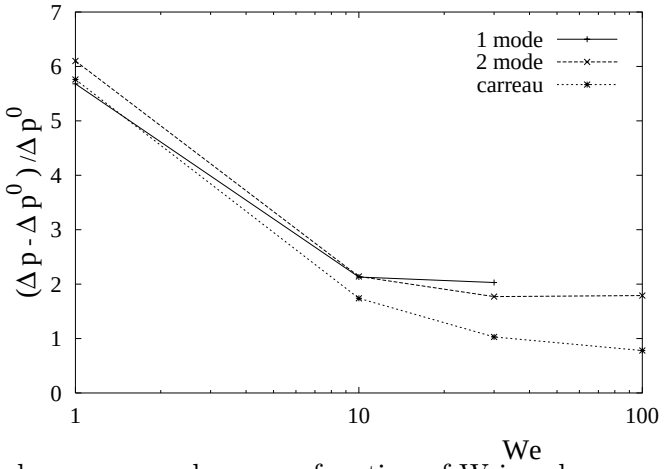

FIG. 15. Dimensionless pressure drop as a function of Weissenberg number for the single- and two-mode DCR models with stretch. We also show results for the inelastic Carreau–Yasuda fit.

The present work shows that chain stretch as implemented in the DCR theory has a dramatic impact on upstream vortex growth in the flow through a constriction. Wapperom and Keunings (2001) made a qualitatively similar observation with the integro-differential pom-pom model for branched polymers. They also observed, however, that the pressure drop in the constriction was not much affected by vortex growth: the pom-pom pressure drop results are indeed practically identical to those obtained with either the MGI model or its Carreau–Yasuda inelastic fit. Following Wapperom and Keunings (2001), we define a dimensionless pressure drop as the ratio $(\Delta p - \Delta p^0)/\Delta p^0$, where Δp is the total pressure drop in the flow domain and Δp^0 corresponds to a fully-developed Poiseuille flow in a tube without the constriction, i.e. of length $40R$ and radius $4R$. The results are plotted in Fig. 15. Although the differences with the inelastic model are larger than for the pom-pom model [Wapperom and Keunings (2001)], they are not qualitatively significant. Since the corresponding experimental data for monodisperse linear polymers are unfortunately not yet available, it is too early at this stage to state that such a puzzling result points to a basic

problem with tube-based theories.

VII. CONCLUDING REMARKS

We have investigated the rheometrical and complex flow response of the DCR differential model with chain stretch. Both a single- and two-mode model was used, with parameter values identified by Ianniruberto and Marrucci (2002) for a monodisperse polybutadiene solution.

While the DCR theory provides satisfactory predictions of shear data in the narrow range of experimental shear rates [Ianniruberto and Marrucci (2002)], it shows anomalous shear-thickening over an intermediate range of (larger) shear rates. The model also predicts that the maximum chain stretch is asymptotically reached in fast shear flows. Whether this particular result is physically realistic is open for debate. The original integro-differential DCR model with stretch, of which the differential version is a mathematical approximation, also predicts anomalous shear-thickening and large stretch in fast shear flows. Moreover, the integro-differential model shows excessive shear-thinning at high shear rates, while its differential approximation remains stable for all shear rates. These results point to the need for further theoretical developments. One common feature of most available tube theories for entangled polymers, including the DCR model, is the use of a decoupling approximation between orientation and stretch. The impact of this approximation is unknown at present, and would deserve a detailed investigation.

Finally, we have performed numerical simulations with the differential DCR model for the start-up flow through an axisymmetric constriction geometry. Significant chain stretch is predicted in the vicinity of the axis of symmetry and in thin boundary layers located at the constriction wall. As a result, the DCR predictions largely depart from the stress-optical rule in these flow regions. Chain stretch also affects the flow kinematics, with the appearance of a large upstream steady-state vortex. Surprisingly, however, the predicted pressure drop is not much affected by these kinematical changes, and it can be described qualitatively by a simple inelastic, shear-thinning model. Since the corresponding experimental pressure data for monodisperse linear polymers are not yet available, it is too early to state that something is missing in the theory in that regard.

ACKNOWLEDGMENTS

This work is supported by the EC TMR contract FMRX-CT98-0210 and the ARC 97/02-210 project, Communauté Française de Belgique. Useful discussions with Ole Hassager and Pino Marrucci are gratefully acknowledged.

REFERENCES

Bird, R. B., R. C. Armstrong and O. Hassager, *Dynamics of polymeric liquids*, vol. 1, John Wiley, New York, 2nd edn. (1987).

Doi, M. and S. F. Edwards, *The theory of polymer dynamics*, Clarendon Press, Oxford (1986).

Guénette, R. and M. Fortin, "A new mixed finite element method for computing viscoelastic flows," J. Non-Newtonian Fluid Mech. **60**, 27–52 (1995).

Ianniruberto, G. and G. Marrucci, "A simple constitutive equation for entangled polymer with chain stretch," J. Rheology **45**, 1305–1318 (2001).

Ianniruberto, G. and G. Marrucci, "A multi-mode CCR model for entangled polymers with chain stretch," J. Non-Newtonian Fluid Mech. **102**, 383–395 (2002).

Larson, R. G., "Convected derivatives for differential constitutive equations," J. Non-Newtonian Fluid Mech. **24**, 331–342 (1987).

Marrucci, G., "Dynamics of entanglements: A nonlinear model consistent with the Cox–Merz rule," J. Non-Newtonian Fluid Mech. **62**, 279–289 (1996).

Marrucci, G., F. Greco and G. Ianniruberto, "Integral and differential constitutive equations for entangled polymers with simple versions of CCR and force balance on entanglements," Rheol. Acta **40**, 98–103 (2001).

Menezes, E. V. and W. W. Graessley, "Nonlinear rheological behavior of polymer systems for several shear-flow histories," J. Polymer Sci.: Polym. Phys. Ed. **20**, 1817–1833 (1982).

Wapperom, P. and R. Keunings, "Simulation of linear polymer melts in transient complex flow," J. Non-Newtonian Fluid Mech. **95**, 67–83 (2000).

Wapperom, P. and R. Keunings, "Numerical simulation of branched polymer melts in transient complex flows using pom-pom models," J. Non-Newtonian Fluid Mech. **97**, 267–281 (2001).

Wapperom, P., R. Keunings and V. Legat, "The backward-tracking Lagrangian particle method (BLPM) for transient viscoelastic flows," J. Non-Newtonian Fluid Mech. **91**, 273–295 (2000).